Published in final edited form as:

Cell Rep. 2023 March 28; 42(3): 112144. doi:10.1016/j.celrep.2023.112144.

Axon targeting of *Drosophila* medulla projection neurons requires diffusible Netrin and is coordinated with neuroblast temporal patterning

Yu Zhang[1], **Scott Lowe**[1], **Andrew Z. Ding**[1], **Xin Li**[1,2,*]

[1]Department of Cell and Developmental Biology, University of Illinois Urbana-Champaign, Urbana, IL 61801, USA

[2]Lead contact

SUMMARY

How axon guidance pathways are utilized in coordination with temporal and spatial patterning of neural progenitors to regulate neuropil assembly is not well understood. We study this question in the *Drosophila* medulla using the transmedullary (Tm) projection neurons that target lobula through the inner optic chiasm (IOC). We demonstrate that the Netrin pathway plays multiple roles in guidance of Tm axons and that temporal patterning of medulla neuroblasts determines pioneer versus follower Tm neurons during this process. Loss of Frazzled (Fra) in early-born pioneer Tm neurons leads to IOC defects, while loss of Fra from follower neurons does not affect the IOC. In the follower projection neurons, Fra is required in other targeting steps including lobula branch extension and layer-specific targeting. Furthermore, different from other identified scenarios of Netrin/Fra involved axon guidance in *Drosophila*, we demonstrate that diffusible Netrin is required for the correct axon targeting and optic lobe organization.

In brief

Zhang et al. find that Netrin pathway plays multiple roles in axon targeting of *Drosophila* medulla projection neurons. It is required in pioneer projection neurons to establish the targeting path and has additional roles in the stepwise targeting of specific projection neurons. Diffusability of Netrin is required in this process.

Graphical Abstract

*Correspondence: lixin@illinois.edu.

AUTHOR CONTRIBUTIONS

Conceptualization, Y.Z. and X.L.; investigation, Y.Z., S.L., and A.Z.D.; formal analysis and visualization, Y.Z.; writing – original draft, Y.Z. and X.L.; writing – review & editing, Y.Z., X.L., S.L., and A.Z.D.; funding acquisition, X.L.

DECLARATION OF INTERESTS

The authors declare no competing interests.

INCLUSION AND DIVERSITY

We support inclusive, diverse, and equitable conduct of research.

SUPPLEMENTAL INFORMATION

Supplemental information can be found online at https://doi.org/10.1016/j.celrep.2023.112144.

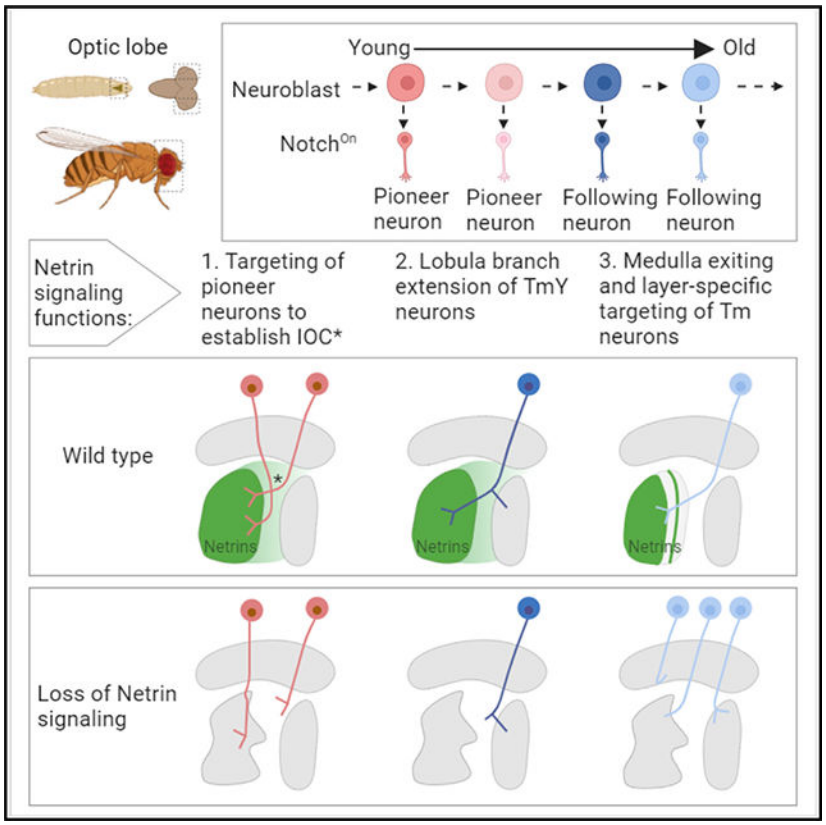

INTRODUCTION

The axons of neurons navigate for a long distance to find their correct targets. Axon guidance cues and their receptors have been identified that play critical roles in this process. The Netrin family of secreted proteins, including UNC-6 in *Caenorhabditis elegans*, Netrin 1–3 in vertebrates, and Netrin A and B in *Drosophila*, play conserved roles in guidance of axons toward and away from the mid-line as well as in guidance of other axons throughout the nervous system.[1] Netrin signaling induces either attraction or repulsion depending on different receptors. Attraction is mainly mediated by the DCC family receptors (Frazzled in *Drosophila*), while repulsion is by the Unc-5 family receptors.[2] As secreted proteins, Netrins have long been considered to be diffusible cues, which direct the targeting of axons over a long distance. However, accumulated studies show that Netrins can also act as short-range haptotactic cues. In mammals, both mechanisms are at play: axons can be guided by long-range Netrins over hundreds of micrometers, while others are guided by Netrins in a contact-dependent manner.[2] However, in *Drosophila*, evidence of long-range action of Netrins has been scarce. A membrane-tethered Netrin construct can fully rescue the mid-line crossing phenotypes of *Drosophila* commissural axons in *Netrin* mutants[3] and can also rescue the targeting layer defect of photoreceptor R8 in the *Drosophila* visual system.[4] In addition, it was shown that with loss of Netrin, R8 axons can still extend to the target layer, but fail to stably attach to it, consistent with short-range contact-dependent

action of Netrin.[5] It is not clear whether Netrins also act as long-range attractive cues in *Drosophila*.

Although Netrin pathway's role in axon guidance has been well described, how it is utilized in different neural types generated by temporal and spatial patterning of neural progenitors to coordinate their targeting and regulate the formation of complex neuropils remains less well understood. In our companion study,[6] we reported that Netrins are required for the assembly of *Drosphophila* optic lobe. Here, we continue to address how the Netrin pathway acts in coordination with temporal patterning to control axon targeting and optic lobe assembly. There are four neuropils in the optic lobe, lamina, medulla, lobula, and lobula plate (Figure 1A). Medulla is the largest neuropil and contains ~800 columns. Each column contains various neural types, and among them, the projection neurons include transmedullary neurons (Tm neurons) and TmY neurons, which extend axons to the next-order neuropils. These neurons can be further divided into unicolumnar (each neuron covers one column) and multicolumnar neurons (each neuron covers more than one column). Tm neurons project from medulla to the different layers of the lobula (Lo1–Lo6), while TmY neurons project from medulla to lobula and lobula plate. Tm neurons project to the lobula in a stereotypic way, with Tm axons from the anterior-most medulla column projecting to proximal-most lobula column, and Tm axons from the posterior-most medulla column to the distal-most lobula column, forming the X-shaped inner optic chiasm (IOC) as a result.[7–10] Electron microscopy (EM) reconstruction of the IOC revealed interleaving bundles and sheets of axons, with axon bundles each containing Tm axons from multiple columns connecting medulla and the lobula complex and axon sheets connecting lobula and lobula plate.[11] When Tm axons from posterior medulla columns leave the bundle, they make a turn to join the sheets of axons, and pass through anterior bundles forming the IOC, to project to lobula.[11]

During development, medulla neurons are generated by medulla neuroblasts that are sequentially transformed from the neuroepithelial (NE) cells at the medial outer proliferation center (OPC). Medulla neuron diversity is achieved mainly by the integration of the spatial and temporal patterning of medulla neuro- blasts and Notch-dependent binary fate choices.[12–14] Temporal patterning is mediated by a cascade of temporal transcription factors (TTFs), including Homothorax (Hth), SoxNeuro (SoxN), Doublesex-Mab related 99B (Dmrt99B), Odd paired (Opa), Eyeless (Ey), Earmuff (Erm), Homeobrain (Hbn), Sloppy-paired (Slp1,Slp2), Scarecrow (Scro), Dichaete (D), BarH1/2, Tailless (Tll), and Glial cell missing (Gcm) in neuroblasts[12,13,15–17] (Figure 1B). These TTFs control the sequential generation of different neural types in different temporal stages, and thus, within a column, there are early-born Tm neural types and late-born Tm types (intra-columnal temporal axis) (Figure 1B). In addition to temporal patterning, the medulla NE is also spatially patterned by transcription factors and signaling pathways.[14] For example, the expression of Visual system homeobox (Vsx) defines the center domain of the medulla NE, and medulla neuroblasts in the center domain generate some types of multicolumnar neurons that later innervate the whole medulla neuropil. In contrast, unicolumnar neurons are generated in all spatial domains of the medulla.[14]

Although significant progress has been made in how various Tm types are generated by neural specification programs in the past few years, how these diverse Tm neurons are integrated to form the organized neuropil is obscure. In our companion study,[6] we reported that Netrins are required for Tm axon guidance through the IOC and that in Tm neurons derived from the Notch-on hemilineage, Notch signaling is required to repress Unc-5 and activate NetB so that Tm neurons can target lobula and provide more NetB to the lobula NetB pool to facilitate targeting of Tm axons from later-born posterior columns. In addition to what was reported in the previous study, we also observed that perturbing the Netrin pathway has pleiotropic phenotypes in Tm targeting. Here, using Tm3 and Tm9 as examples, we demonstrate that the Netrin pathway functions at multiple steps of Tm axon targeting, and this process is coordinated with temporal and spatial patterning of neuronal specification. First, Frazzled (Fra) is required non-cell autonomously for Tm3 axons to leave the medulla neuropil, and a multicolumnar TmY neuron generated in the center domain and possibly others function in this process. Second, Fra functions in early-born Tm neurons generated in the Opa temporal stage to pioneer the IOC, which is essential for later-born Tm neurons to target correctly. Finally, Fra is required cell autonomously for layer-specific targeting of Tm neurons that terminate at the NetB-enriched lobula layers. Furthermore, we show that the membrane-tethered Netrin cannot fully rescue the IOC defect and the targeting layer defect of Tm axons, providing evidence that the diffusibility of Netrin is required for targeting of visual projection neurons and optic lobe organization in *Drosophila*.

RESULTS

Tm3 and Tm9 axons target lobula in a temporal process

We used two examples of Tm neurons: Tm3, which targets lobula layer 4, and Tm9, which targets lobula layer 1 (Figure 1A) to further characterize the pleotropic roles of Netrin signaling in Tm axon targeting. Both Tm3 and Tm9 express the transcription factor Drifter (Dfr) and are generated in the Ey stage, with Tm9 born earlier than Tm3.[12,13,17,18] We first traced Tm3 and Tm9 axon targeting and NetB distribution through development. Tm axon targeting can be divided into several steps: they need to first navigate down through the medulla neuropil, leave the medulla neuropil in axon bundles, make a turn to target lobula, and pass through anterior axon bundles, thus forming the IOC, and finally terminate at their specific target layer. There is a temporal gradient of Tm axon targeting with Tms from anterior medulla columns targeting the proximal lobula columns first, followed by Tms from posterior medulla columns targeting the distal lobula columns. At 24% APF (after puparium formation), Tm3 axons from posterior medulla columns have not arrived at the distal columns of the lobula, and the most posterior Tm3 axons have not left the medulla neuropil. All the arrived ones in the proximal lobula columns show the bushy growth cone structure (Figure 1C). In contrast, all born Tm9 axons have reached the lobula (Figure 1D). Therefore, in each lobula column, the Tm3 axon arrives at the lobula later than Tm9. In addition, we also observed a progressive axon terminal maturation of Tm9 at 24% APF. We found that while Tm9 axons at the distal columns exhibit the bushy growth cone structure (Figure 1D1), indicative of active axon targeting, those at the proximal columns already have the mature cylinder-like axon terminals as in the adult stage (Figure 1D2). Altogether, these data indicate that within a column, Tm neurons project to lobula in a temporal sequence.

Among columns, axon terminals mature progressively, with those at proximal (old) lobula columns maturing early and those at distal (young) columns maturing late.

At 24% APF, NetB is distributed almost throughout the whole lobula neuropil, with a higher concentration at superficial layers than at deep layers (Figure 1E). Moreover, we observed a gradient of NetB in the cleft (arrows in Figure 1E) through which Tm bundles target lobula. Tm3 growth cones are localized in high NetB layers (Figure 1C). For young Tm9 in distal lobula columns, their growth cones also colocalize with NetB (Figure 1D1). In contrast, for old Tm9 in proximal lobula columns, their cylinder-like axon terminals do not colocalize with NetB (Figure 1D2), suggesting that the dynamic distribution of NetB has already started at this stage.

At 48% APF when lobula layers are forming, NetB was distributed and finally enriched in two regions in the lobula, one thin layer at Lo2 and one big domain at Lo4–Lo6. All Tm3 axons have arrived at the lobula, and they have arborizations at two lobula layers, Lo2 and Lo4, both of which are enriched for NetB (Figures 1F and 1H). In contrast, all Tm9 axons exhibit the cylinder-like axon terminals at Lo1 (Figure 1G), which is devoid of NetB. Therefore, at the layer-targeting step, Tm3 layer-specific targeting coincides with NetB enrichment, while Tm9 axons target at superficial lobula layer where NetB is not enriched.

Before examining the role of Netrin signaling in Tm3/Tm9 axon targeting, we first validated the expression patterns of two Netrin receptors, Fra and Unc-5. We identified a Tm3-specific Gal4 driver (GMR12C11-GAL4) that starts expression at the late third larval stage. The identity of labeled neurons was confirmed by staining with Tm3 identity markers (Dfr and Cut) (Figures S1A and S1A1)[18] at the early pupal stage and by costaining with existing Tm3-lexA[19] at the adult stage (Figures S1B and S1B2). Consistent with our companion study,[6] we verified that most Tm3 and Tm9 neurons examined express Fra (Figures 1I–1I2 and 1K–1K2) but not Unc-5 (Figures 1J and 1L) at 24% APF.

Fra is required non-cell-autonomously for Tm3 axons to leave the medulla neuropil

We next examined how loss of Netrin signaling affected Tm3 targeting by knocking down Fra. We utilized MARCM with a well- studied loss-of-function *fra* allele, *fra3*.[20] We observed various targeting defects of Tm3, including stalling at medulla layer 10 (M10), mistargeting to superficial lobula layers or the lobula plate (Lop) (Figures 2B, 2G, and 2H), suggesting that Netrin signaling may affect multiple steps of Tm3 targeting. Consistently, we found in *netrin* double-mutant $netAB^{\Delta}$, 76.7% of Tm3 axons do not leave the medulla neuropil (Figures 2D, 2G, and 2H). In contrast, in $netAB^{\Delta}$ mutants, Tm9 axons leave the medulla nor mally and terminate at the correct Lo1 layer despite the failure to form the IOC (Figure 2D in companion study[6]). Therefore, Tm3 and Tm9 have a distinct requirement of Netrin signaling for leaving the medulla neuropil. To better view the morphology defects of Tm3, we labeled individual Tm3 neurons using Multi- color Flpout (MCFO).[9] We found that most Tm3 axons did not innervate lobula in $netAB^{\Delta}$ mutants. Instead, they were stalled at M10 and turned back to the medulla, forming a hook-like structure similar to Mi1 (Figures 2F and 2G). Altogether, these data suggest that the first step of Tm3 axon targeting that re- quires the Netrin pathway is to leave the medulla neuropil.

As shown before, most Tm3 axons do not leave the medulla in *netrin* mutants, and a small percentage do not leave the medulla in *fra* mutant MARCM clones. Since we used *Tm3-Gal4* instead of ubiquitous Gal4s to label the mutant MARCM clone, the invisible *fra* mutant clone size may vary. We hypothesized that Tm3 axons surrounded by big *fra* mutant clones were stalled at M10, meaning that Fra is required non-cell-autonomously in surrounding cells to help Tm3 axons leave the medulla. To find which neural types were involved, we checked Tm3 targeting by knocking down Fra with Gal4 drivers expressed in multiple cell types. We found that 44% of Tm3 neurons are stalled at M10 when Fra is knocked down using *dfr-Gal4* (Figures 2J and 2L) and that 72% of Tm3 are stalled at M10 when using *DIP-eta-Gal4* (Figures 2K and 2L), suggesting that neurons that help Tm3 leaving the medulla are within these Gal4-expressing cells.

A previous study showed that *dfr-Gal4*-labeled neurons include Mi10b, Tm3a, Tm3b, Dm8a, Dm8b, Tm9, TmY3, Tm27, and Tm27Y.[18] *DIP-eta-Gal4* is expressed in Mi9, Mi10, Tm2, Tm3, Tm5c, TmY3, and TmY13.[21] Combining these data, only Mi10, Tm3, and TmY3 are labeled by both Gal4 lines. Since Mi10 axons do not leave the medulla, TmY3 is likely essential for Tm3 to leave the medulla. If so, the axon guidance of TmY3 should also be regulated by Fra. Since the TmY3-specific early driver is not available currently, we labeled individual TmY3 by crossing *DIP-eta-Gal4* with MCFO. We found that Tm2 and TmY3 are the most frequently labeled neurons (Figures 2M and S2A). In the wild type, each TmY3 axon bifurcates into two branches, with one branch turning toward the lobula and the other projecting to the Lop (Figures 2M and 2P). Interestingly, after knocking down Fra, the lobula branch of TmY3 becomes tiny and points to the Lop (Figures 2N–2P). In contrast, the Lop branch and medulla arborization remain normal (Figures 2N–2P), indicating that Fra is required for the lobula branch of TmY3 to target the lobula neuropil. Moreover, we found that Tm2 axons leave the medulla and target lobula normally when Fra is knocked down with *DIP-eta-Gal4* (Figure S2B). Therefore, our data suggest that TmY3 likely helps Tm3 to leave the medulla neuropil. Since we currently do not have specific drivers for TmY3, Tm27, Tm27Y, Tm5c, or TmY13, we cannot validate whether Fra acts cell autonomously for the lobula branch extension of TmY3 and whether TmY3 is the only required neural type that guides Tm3 leave the medulla neuropil. However, our data raised the possibility that without Fra, TmY3 cannot extend the lobula branch, and as a result, Tm3 is less likely to leave the medulla neuropil. TmY3 expresses Dfr[18] and is generated in the same temporal stage as Tm3, but TmY3 also expresses Vsx2 (Figure S2E) and should be a type of multicolumnar neuron generated in the center domain.[14,15] How TmY3 helps Tm3 leave the medulla neuropil remains to be further studied. To examine if Tm3 axons initially leave the medulla but retract back, similar to what was observed in R8,[5] we examined Tm3 targeting in 24% APF brains in which Fra was knocked down using *dfr-Gal4*. We found that even at this stage, when Tm3 axons from posterior columns are still actively targeting, most Tm3 axons do not leave the medulla (Figure S2D), suggesting that the initial leaving step has defects.

Fra expressed in early-born Tm neurons within each column is required for the formation of the inner chiasm

After leaving the medulla neuropil, Tm axons turn toward the lobula through the IOC. As shown previously, a small fraction of Tm3 axons leave the medulla when knocking down Fra by *drf-Gal4*, and they enter the IOC normally (Figure 2J), ruling out the possibility that Fra is required cell autonomously for Tm3 axons to join the IOC. In contrast, in $netAB^{\Delta}$ mutants, the Tm3 axons that leave the medulla do not form the X-shaped IOC but cut through the lobula neuropil (arrow in Figure 2D), consistent with our previous observation that Netrin signaling does contribute to IOC formation.

Tm neurons are generated in a temporal sequence. We found that they also projected sequentially, as exemplified by early-born Tm9 projecting earlier than late-born Tm3 (Figures 1C and 1D). Therefore, it is less likely that all Tm axons contribute equally to IOC formation. We speculated that a specific subset of Tm neurons should be crucial for IOC formation. We first used Gal4 drivers initiated in neuroblasts of different temporal windows (Figure 1B) to knock down Fra in their progenies. Medulla neuroblasts sequentially generate different neural types in different temporal windows marked by a TTF cascade: Hth → Opa → Ey+Erm → Ey+Opa → Slp → D → B-H1&2 → Tll → Gcm.[15–17] We found that knocking down Fra using *ey-Gal4*, *slp-Gal4*, or $D\text{-}Gal4^{22}$ did not affect the inner chiasm formation (Figures S3A–S3D and 3N), indicating that Fra expressed in Tm neurons born during and after the Ey window is not necessary for the formation of the inner chiasm.

Another TTF Opa is expressed in two temporal windows, with the first one before the Ey stage and the second one in the late Ey stage (Ey+Opa temporal stage)[17] (Figures 1B and 3N). Neuroblasts in the first Opa window generate neurons expressing Runt (Ap^{-}, Notch-off hemilineage).[20] Opa is also required to generate TfAP-2-expressing neurons (Ap^{+}, Notch-on hemilineage, which include Tm1, Tm2, Tm4, and Tm6).[15,23,24] However, it was not clear whether all four Tm neurons were born in the first Opa temporal stage (Figure 1B). In addition, TfAP-2 is also expressed in Pm1/2/3 neurons (Proximal medulla neurons marked by transcription factor Svp) generated in the Hth temporal window[14,23] (Figures 1B and 3A–3A2). We found a TfAP-2 driver (GMR24B02-GAL4) that shows expression at the third-instar larval stage in the Flylight Gal4 collection. We characterized this driver and found that it was indeed expressed in the three stripes of TfAP-2^{+} medulla neurons (Figure S3E–S3E2). The first stripe includes the Svp^{+} Pm1/2/3 neurons (big arrow in Figures 3B–3B3, 3C, and 3C1). The second stripe of TfAP-2^{+} neurons are intermingled with $Runt^{+}$ neurons (small arrow in Figures 3B–3B3), born before Tm9 (small arrow in Figures 3C and 3C1), and not labeled by Ey-Gal4>LacZ (small arrow in Figures 3E and 3E1), suggesting that they are generated in the first Opa temporal window. The third stripe of TfAP-2^{+} neurons are intermingled with the first layer of Toy^{+} neurons (arrowhead in Figures 3C and 3C1) and are labeled by Ey-Gal4>LacZ (arrow-head in Figures 3E and 3E1), suggesting that they are born in or after the Ey stage. The third stripe of TfAP2-expressing neurons was still generated in *slp* mutant clones (Figures 3D and 3D1) but was lost when we specifically knocked down the second Opa stripe using *ey-gal4* driving *opa-RNAi*, indicating that these neurons were born during the second Opa (Opa+Ey) temporal window (Figures 3F, 3F1, and 3N).

When Fra was knocked down using *TfAP-2-Gal4*, IOC formation, labeled by axons of Tm3, which does not express TfAP2, was disrupted (Figure 3H). Similarly, knocking down TfAP-2 with *tll-gal4* also caused a severe disruption of the IOC marked by Tm3 axons (Figure 3I). The knockdown efficiency of *UAS-TfAP-2RNAi* was confirmed by anti-TfAP2 staining (Figures S3F and S3G). To exclude a possible role for Pm1/2/3 neurons in IOC formation, we knocked down Fra in Pm1/2/3 neurons using a *svp-Gal4* (that mimics the Svp expression pattern) (Figures 3A–3A2). We found that this does not affect IOC formation (Figure 3J) as expected because Pm neurons do not project outside of the medulla. Thus, Fra is required in TfAP2-expressing Tm neurons (Tm1, Tm2, Tm4, Tm6) for IOC formation.

To further narrow down the Tm neuron types required for IOC formation, we utilized Tm1, Tm2, Tm4, and Tm6 specific markers[24] to examine the temporal windows in which they are generated. At mid-pupal stages, in addition to TfAP2, Tm1 also expresses Drgx (Figures S3H–S3H4), Tm2 expresses Pdm3 and Mef2 (Figures S3I–S3I6), and both Tm4 and Tm6 still express Aop, but only Tm6 expresses SoxN (Figures S3J–S3J8).[24] Using *ey-Gal4* lineage tracing, we found Tm1 and Tm4 are not labeled with *ey-Gal4* (Figures S3H–S3H4 and S3J–S3J8) and thus should be born before the Ey stage (Figure 3N), while Tm2 and Tm6 are labeled with *ey-Gal4* (Figures S3I–S3I6 and S3J–S3J8) and should be born during or after the Ey stage (Figure 3N). We also confirmed the Notch status of these neurons: in *Su(H)* mutant clones, the second and third stripes of TfAP2 (expressed in Tm1, Tm4, Tm2, and Tm6) are lost, while TfAP2 expressed in Pm neurons (first stripe) are still present (Figures 3L–3M1). Taken together, our data suggest that Tm1 and Tm4 are the Notch-on neurons born in the first Opa window (second TfAP2 stripe), while Tm2 and Tm6 are the Notch-on neurons born in the second Opa (Ey+Opa) window (third TfAP2 stripe) (Figure 3N).

Knocking down TfAP2 using *ey-Gal4* did not cause any phenotype (Figure 3K), suggesting that Tm2 and Tm6 are not required for IOC formation. Knocking down Fra specifically in Tm1 (Figure S2B of companion study[6]) or Tm4 (shown later in Figure 4H) alone did not cause a defect in IOC formation, indicating that loss of Fra from these two individual Tm types does not affect IOC formation. Because of a lack of a specific driver expressed in both Tm1 and Tm4, we could not directly test whether knocking down Fra or TfAP2 in both Tm1 and Tm4 affects IOC formation. Nevertheless, taken together, our results suggest that a group of early-born TfAP-2-expressing Tm neurons act redundantly for IOC formation through Fra, and most likely, Tm1 and Tm4 neurons generated in the first Opa temporal window are the pioneering axons. These pioneering axons require Fra to construct the skeleton of IOC, thus building the axon targeting path. Axons of late-born neurons such as Tm3 join the IOC, extend along the targeting path, and reach the lobula neuropil. During this step, Fra does not act cell autonomously in Tm3.

Fra acts cell-autonomously for Tm axons to target deep lobula layers

After reaching the lobula, Tm axons need to terminate at the correct lobula layers. We found that knocking down Fra specifically in Tm3 resulted in its mistargeting to superficial lobula layers (from Lo2 to the superficial half of Lo4) or the Lop (Figure 4B), suggesting that Fra acts cell autonomously for Tm3 axons to target the correct layer. We also noticed that

Tm3 axons leave the medulla and join the IOC normally when knocking down Fra in Tm3 specifically, consistent with our previous conclusion that Fra acts non-cell autonomously in these first two steps. Besides Tm3, Tm4 axons also terminate at Lo4. Therefore, we examined whether Tm4 axons also utilize Fra for their layer-specific targeting. After knocking down Fra, 72% of Tm4 axons did not reach the normal termination layer but instead stalled at more superficial lobula layers (from Lo2 to the superficial half of Lo4) or mistargeted to the Lop (Figure 4H), suggesting that the requirement of Netrin signaling to target lobula layer 4 is likely to be a common principle. In contrast, targeting of Tm9 axons to the superficial lobula layer 1, which is devoid of NetB, is not affected when Fra is knocked down (companion paper's Figure S2B).

Netrin isoforms and diffusibility are required differently in each step of Tm3 axon targeting

Since there are two isoforms of Netrins in *Drosophila*, NetA and NetB, we next examined how they are required in each step of Tm axon targeting. In *netA* mutants, Tm3 and Tm4 targeting is normal (Figures 4C and 4I). In contrast, in *netB* mutants, 55.4% of Tm3 and 60% of Tm4 axons stalled at more superficial lobula layers (Figures 4D and 4J), despite leaving the medulla neuropil and joining the IOC normally. Therefore, NetA and NetB act redundantly for Tm axons to leave the medulla and for IOC formation, while NetB alone is necessary for the targeting layer specificity of Tm3 and Tm4. These results are consistent with our findings that NetA is enriched more strictly in the cleft, while NetB is localized to both the cleft and the lobula neuropil.

Finally, we tested if the diffusibility of Netrins is required at each step of Tm axon targeting. We first validated that NetB distribution was affected in $netA^{\Delta}netB^{TM}$ flies in which NetB could not diffuse because it was attached to a membrane-bound domain.[3] At 24% APF, NetB is localized in the lobula and the surface of the Lop (Figure 4M), compared with the lobula-only NetB distribution in wild type (Figure 4L). At 48% APF, NetB is broadly localized to the whole lobula and part of the Lop (Figure 4O). Then, we examined if this membrane-tethered NetB could rescue targeting of Tm axons. We found that all Tm3 axons left the medulla normally, and about 70% of Tm3 and Tm4 were mistargeted either at superficial lobula layers or the Lop in adult $netA^{\Delta}netB^{TM}$ flies (Figures 4E and 4K). In addition, some Tm3 and Tm4 axons do not join the IOC in adult $netA^{\Delta}netB^{TM}$ flies. In contrast, $netA^{\Delta}netB^{TM}/netA^{+}netB^{+}$ brains do not have any phenotype (Figure 4F), validating that the phenotype is caused by loss of NetB secretion and not by gain of an inappropriate interaction by $netB^{TM}$. Taken together, these data indicate that diffusible NetB is not required for Tm3 to leave the medulla but is required for IOC formation and layer-specific targeting of Tm neurons that terminate at NetB enriched layers.

DISCUSSION

Netrin signaling has multiple roles in the optic lobe organization

In the *Drosophila* optic lobe, Tm neurons are medulla projection neurons that connect medulla with a higher-order neuropil, lobula. Our companion study[6] and this study demonstrate that Netrin signaling is reiteratively used in multiple targeting steps of Tm neurons and contribute to optic lobe organization (Figure 5). First, at the early pupal stage,

Netrins are enriched in the cleft and the lobula, which is required for Tm axons from late-born medulla columns to cross all axons from early-born medulla columns and form the IOC, creating the base for a retinotopic map. In wild-type optic lobe, the lobula layers are running perpendicular to medulla layers due to the formation of the IOC. With loss of Netrin signaling, the IOC is disrupted, and the relative orientation of lobula vs. medulla is changed to almost parallel. Furthermore, the lobula is fragmented because the later-born Tm axons failed to cross anterior axon bundles and mistarget to the surface of the Lop. Then, at the mid-pupal stage, NetB is enriched at specific lobula layers, and regulates layer-specific targeting of Tm axons that terminate at the NetB-enriched layers. Therefore, Netrin signaling is utilized in IOC formation and layer-specific targeting sequentially. Furthermore, in TmY projection neurons that send bifurcated axons to target two higher-order neuropils, lobula, and the Lop, our results suggest that Netrin signaling is specifically required for the extension of the lobula branch, but not for the Lop branch.

Coordination of temporal patterning with Netrin-/Fra-dependent axon guidance

Each medulla column consists of multiple types of Tm neurons, which are generated chronologically directed by temporal patterning of medulla neuroblasts. How these Tm neurons contribute to IOC formation was not clear. Do all Tm neurons contribute equally to IOC formation, or do some neurons act as pioneers to build the IOC skeleton and others follow the path of these pioneers? By knocking down Fra in neurons born at different temporal windows, we found that loss of Fra in all neurons born in Ey and later stages does not affect IOC formation. In contrast, loss of Fra in early-born TfAP-2-expressing Tm neurons causes defects in IOC formation as assessed using later-born Tm neurons, although these later-born Tm neurons do still express Fra. Thus, our results suggest that the TfAP-2-expressing early-born Tm neurons generated in the first Opa temporal stage are likely to be the pioneering axons for the initial establishment of the IOC (Figure 5). Therefore, temporal patterning determines the leader vs. follower in the Netrin-/Fra-dependent guidance of Tm axons.

Our lineage-tracing study suggests that pioneer neurons are likely Tm1 and Tm4. Both have the properties of being a pioneer neuron. First, they are the first-born Tm neural types within each lineage. Therefore, they can target their axons early and establish the targeting path for late-born Tm neurons. Second, they are unicolumnar neurons, with one each in every medulla column serving as the leader to guide late-born neurons. Not surprisingly, we found that when the IOC shows defect, all following Tm neurons follow the wrong targeting path. What's more, Tm1 and Tm4 act redundantly as pioneer neurons, adding robustness to the essential process of IOC formation.

Tm3 has a special requirement for Netrin signaling to leave the medulla

In *netrins* double mutants, most Tm3 axons do not leave the medulla neuropil, while axons of Tm9 neurons do leave. Therefore, Netrin signaling is specifically required for the leaving of Tm3 axons from the medulla before joining the IOC. However, Fra is not needed cell autonomously for the leaving of Tm3 axons from medulla. Instead, Tm3 needs help from other neuron types whose targeting should also be regulated by Netrin signaling. TmY3 is likely to be the neuron that helps Tm3 leave the medulla. Without Fra, TmY3 lost its

innervation of lobula, showing a tiny neurite at the branching point. How losing the lobula branch of TmY3 affects Tm3 leaving the medulla is not clear. Since Tm3 outnumbers TmY3, with a ratio of 11:4,[25] TmY3 may not guide Tm3 to leave the medulla by physical interaction. Interestingly, TmY3 is generated in the same temporal stage as Tm3 but only in the center domain of the medulla. Whether this is relevant to the mechanism by which TmY3 helps Tm3 leave the medulla remains to be studied.

Netrin diffusibility is differently required in each step of axon targeting

Previous studies found that in R8 axon targeting, Netrins are synthesized by M3-targeting neuron L3, and as a result, their diffusion is not required for R8 axon targeting.[5,26] However, in our case, we found that NetB diffusion is required at multiple steps of Tm axon targeting, including IOC formation and layer-specific targeting of Tm neurons that target NetB-enriched layers. Our results indicate that NetB gradients are formed by NetB diffused from long-range sources and enriched by local Fra and other potential factors.[27] Indeed, we observe a low-to-high NetB gradient on the IOC targeting path toward the lobula at the axon targeting stage (24% APF), but this gradient is no longer observed at 48% APF when targeting is complete. Our study raises the possibility that NetB diffused from lobula forms a gradient that guides Tm axons to turn toward lobula and form the IOC. However, even in *Netrin* null mutants, there is still incomplete penetrance in Tm axon targeting defects. It is also possible that Fra may promote the stable attachment of the growth cone to the substrate-bound Netrin gradient, which provides traction force for Tm axons to move toward the lobula similar to what was proposed in a previous study.[5] In summary, our study demonstrates that the *Drosophila* visual projection neurons require diffusible Netrin to turn toward its targeting neuropil and later for layer-specific targeting.

Limitations of the study

We demonstrate that Fra is required in TfAP2-expressing neurons to pioneer the IOC, and our data suggest that among the TfAP2-expressing neurons, Tm1 and Tm4 may act redundantly in this role. However, currently, we do not have an early driver that is expressed in both Tm1 and Tm4 but not in other neurons. In addition, we do not have specific early drivers for TmY3 and were not able to test if Fra acts cell autonomously for the lobula branch extension of TmY cells and if TmY3 alone is responsible for helping Tm3 to leave the medulla.

STAR★METHODS

RESOURCE AVAILABILITY

Lead contact—Further information and requests for resources and reagents should be directed to and will be fulfilled by the lead contact, Xin Li (lixin@illinois.edu).

Materials availability—This study did not generate new unique reagents.

Data and code availability

- This paper analyzes existing, publicly available data. These accession numbers for the datasets are listed in the key resources table. The published scRNA-seq

data of 3rd and 15% APF optic lobe cells were downloaded from NCBI GEO: GSE167266. Microscopy data reported in this paper will be shared by the lead contact upon request.

- This paper does not report original code.
- Any additional information required to reanalyze the data reported in this paper is available from the lead contact upon request.

EXPERIMENTAL MODEL AND SUBJECT DETAILS

Fly stocks—Fly stocks were maintained in standard medium at 25°C except for RNAi experiments, for which crosses were grown at 29°C. The following stocks/crosses were used for expression analyses: *fra-GFP* (BL 59835); *unc-5-GFP* (BL 64547); *UAS-myr-mRFP* (BL7118); *Tm9-Gal4* (BL 48050); *Tm3-Gal4*(BL48569) for adult labeling; *Tm3-Gal4* (BL76324) for larva labeling; *Tm4-Gal4* (BL49922); *Tm3-lexA* (BL52459), *lexopTdTomato*. The following stocks/crosses were used for loss of function with mutants: $netA^{\Delta}$, $netB^{\Delta}$, $netA^{\Delta}B^{TM}$ and $netA^{\Delta}B^{\Delta}$ (from B. J. Dickson); *MCFO* (BL64085). The following stocks/crosses were used with UAS-RNAi: *UAS-fraRNAi* (BL 40826); *UAS-TfAP2-RNAi* (VDRC 101552); *UAS-Opa-RNAi* (VDRC 101531); *tll-Gal4* (GMR31H09, BL 49694); *dfr-Gal4* (from M. Sato); *DIP*-h-*Gal4* (BL 90318); *SoxN-Gal4* (GMR41H10Gal4); *Tm9-lexA* (BL54982); *ey-Gal4* (GMR16F10, BL48737); *slp-Gal4* (GMR35H02, BL 49923); *D-Gal4* (GMR12G08, BL47855).

METHOD DETAILS

Immunostaining and antibodies—Wandering 3rd instar larvae were picked for larval stage immunostaining. White pupae were growing to certain age either in a Petri dish layered with hydrated filter paper when growing at 25°C or in a vial of food at 29°C. The pupal stage lasts about 100 hr when growing at 25°C and about 78 hr at 29°C. As a result, 24% APF means growing white pupae for 24 hours at 25°C and about 19 hours at 29°C. Immunostaining was done as described previously[12] with a few modifications. Brains were dissected in phosphate-buffered saline (PBS), fixed for 30 min for the 3rd instar larvae, 40 min for pupae and adult at room temperature in 4% paraformaldehyde in PBS, washed in PBS containing 0.3% Triton X-100. Brains were then incubated in primary antibody solution at 4°C overnight, washed three times with PBST, incubated in secondary antibody solution at room temperature for 3 hours, washed three times with PBST and three times with PBS and mounted in Slowfade.

The following primary antibodies were used: rabbit anti-NetB (from B.Altenhein, 1:100), sheep anti-GFP (AbD Serotec: 4745–1051, 1:500), Phalloidin-iFluor 405 (Abcam: ab176752, 1:1000), rabbit anti-RFP (Abcam: ab62341, 1:1000), rat anti-Dfr (from M. Sato, 1:100), mouse anti-Cut (DSHB:2B10, 1:10), guinea pig anti-Toy (from C. Desplan, 1:200), guinea-pig anti-Runt (from C. Desplan, 1:500), guinea pig anti-TfAP-2 (from C. Desplan, 1:100), rat anti-Drgx (from C. Desplan, 1:250), rat anti-Pdm3 (from C. Desplan, 1:1000), rabbit anti-Mef2 (from C. Desplan, 1:250), mouse anti-Aop/Yan (DSHB: 8B12H9, 1:100), mouse anti-Myc (DSHB: 9E10, 1:10), rabbit anti-HA (CST #3724, 1:1500),

rat anti-Flag (Novus: NBP1–06712, 1:100), Mouse anti V5-Tag:DyLight-550 (Bio-Rad: MCA1360D550GA, 1:800), rat anti-DN-cadherin (DSHB: DN-Ex#8, 1:50).

Secondary antibodies were from Jackson or Invitrogen. Images are acquired using a Zeiss Confocal Microscope. Figures are assembled using Photoshop and Illustrator.

Generate MARCM clones—To generate wild-type or *fra* mutant MARCM clones, flies of *ywhsFLP UASCD8GFP; FRT G13/Cyo; Tm3-Gal4/TM6B* were crossed with *FRTG13* or *FRTG13*, *fra3* (BL8813). To generate *slp* mutant MARCM clones, flies of *y,w,hsFLP,UAS-CD8::GFP; FRT40A, tub-Gal80; tub-Gal4/TM6B* were crossed with *FRT40A, slp*^{S37A}*/SM6-TM6B* flies (Gift from Andrew Tomlinson).[28] To generate wild-type or *Su(H)* mutant MARCM clones, flies of *y,w,hsFLP,UAS-CD8::GFP; FRT40A, tub-Gal80; tub-Gal4/TM6B* were crossed with *FRT40A* or *FRT40A, Su(H)*$^{\Delta 47}$*/CyO* flies (gift from F. Schweisguth). To induce mutant clones, the progenies were heat-shocked at 37°C for 1 hour at early larval stage and dissected at adult or 30% APF.

QUANTIFICATION AND STATISTICAL ANALYSIS

From the targeting defect: at least five brains were imaged, and in each brain numbers of axon terminals from at least three different focal planes were counted.

Supplementary Material

Refer to Web version on PubMed Central for supplementary material.

ACKNOWLEDGMENTS

We thank the fly community, especially Greg J. Bashaw, Benjamin Altenhein, Barry J. Dickson, and Claude Desplan, for generous gifts of antibodies and fly stocks. We thank the Bloomington Drosophila Stock Center, the Vienna Drosophila RNAi Center, the Developmental Studies Hybridoma Bank, and TriP at Harvard Medical School (NIH/NIGMS R01-GM084947) for fly stocks and reagents. We thank Filipe Pinto-Teixeira, Isabel Holguera, and Neset Ozel for helpful discussions. This work was supported by National Institutes of Health (Grant 1 R01 EY026965–01A1 and 2 R01 EY026965–06A0 to X.L.).

REFERENCES

1. Sun KLW, Correia JP, and Kennedy TE (2011). Netrins: versatile extracellular cues with diverse functions. Development 138. 10.1242/dev.044529.
2. Tessier-Lavigne M (2020). Axon guidance: netrins. In Cellular Migration and Formation of Axons and Dendrites, pp. 87–108. 10.1016/B978-0-12-814407-7.00004-3.
3. Brankatschk M, and Dickson BJ (2006). Netrins guide Drosophila commissural axons at short range. Nat. Neurosci. 9, 188–194. 10.1038/nn1625. [PubMed: 16429137]
4. Timofeev K, Joly W, Hadjieconomou D, and Salecker I (2012). Localized netrins act as positional cues to control layer-specific targeting of photoreceptor axons in Drosophila. Neuron 75, 80–93. 10.1016/J.NEURON.2012.04.037. [PubMed: 22794263]
5. Akin O, and Zipursky SL (2016). Frazzled promotes growth cone attachment at the source of a netrin gradient in the Drosophila visual system. Elife 5, e20762. 10.7554/eLife.20762.001. [PubMed: 27743477]
6. Zhang Y, Lowe S, Ding AZ, and Li X (2023). Notch dependent binary fate choice regulates Netrin pathway to control axon guidance of Drosophila visual projection neurons. Cell Reports. 10.1016/j.celrep.2023.112143.

7. Fischbach KF, and Dittrich APM (1989). The optic lobe of Drosophila melanogaster. I. A Golgi analysis of wild-type structure. Cell Tissue Res. 258, 441–475. 10.1007/BF00218858.
8. Morante J, and Desplan C (2008). The color-vision circuit in the medulla of Drosophila. Curr. Biol. 18, 553–565. 10.1016/J.CUB.2008.02.075. [PubMed: 18403201]
9. Nern A, Pfeiffer BD, and Rubin GM (2015). Optimized tools for multicolor stochastic labeling reveal diverse stereotyped cell arrangements in the fly visual system. Proc. Natl. Acad. Sci. USA 112, E2967–E2976. 10.1073/PNAS.1506763112. [PubMed: 25964354]
10. Ngo KT, Andrade I, and Hartenstein V (2017). Spatio-temporal pattern of neuronal differentiation in the Drosophila visual system: a user's guide to the dynamic morphology of the developing optic lobe. Dev. Biol. 428, 1–24. 10.1016/J.YDBIO.2017.05.008. [PubMed: 28533086]
11. Shinomiya K, Horne JA, McLin S, Wiederman M, Nern A, Plaza SM, and Meinertzhagen IA (2019). The organization of the second optic chiasm of the Drosophila optic lobe. Front. Neural Circuits 13, 65. 10.3389/fncir.2019.00065. [PubMed: 31680879]
12. Li X, Erclik T, Bertet C, Chen Z, Voutev R, Venkatesh S, Morante J, Celik A, and Desplan C (2013). Temporal patterning of Drosophila medulla neuroblasts controls neural fates. Nature 498, 456–462. 10.1038/nature12319. [PubMed: 23783517]
13. Suzuki T, Kaido M, Takayama R, and Sato M (2013). A temporal mechanism that produces neuronal diversity in the Drosophila visual center. Dev. Biol. 380, 12–24. 10.1016/J.YDBIO.2013.05.002. [PubMed: 23665475]
14. Erclik T, Li X, Courgeon M, Bertet C, Chen Z, Baumert R, Ng J, Koo C, Arain U, Behnia R, et al. (2017). Integration of temporal and spatial patterning generates neural diversity. Nature 541, 365–370. 10.1038/nature20794. [PubMed: 28077877]
15. Konstantinides N, Holguera I, Rossi AM, Escobar A, Dudragne L, Chen YC, Tran TN, Martírez Jaimes AM, Özel MN, Simon F, et al. (2022). A complete temporal transcription factor series in the fly visual system. Nature 604, 316–322. 10.1038/s41586-022-04564-w. [PubMed: 35388222]
16. Tang JLY, Hakes AE, Krautz R, Suzuki T, Contreras EG, Fox PM, and Brand AH (2022). NanoDam identifies homeobrain (ARX) and Scarecrow (NKX2.1) as conserved temporal factors in the Drosophila central brain and visual system. Dev. Cell 57, 1193–1207.e7. 10.1016/J.DEVCEL.2022.04.008. [PubMed: 35483359]
17. Zhu H, Zhao SD, Ray A, Zhang Y, and Li X (2022). A comprehensive temporal patterning gene network in Drosophila medulla neuroblasts revealed by single-cell RNA sequencing. Nat. Commun. 13, 1247. 10.1038/s41467-022-28915-3. [PubMed: 35273186]
18. Hasegawa E, Kitada Y, Kaido M, Takayama R, Awasaki T, Tabata T, and Sato M (2011). Concentric zones, cell migration and neuronal circuits in the Drosophila visual center. Development 138, 983–993. 10.1242/dev.058370. [PubMed: 21303851]
19. Behnia R, Clark DA, Carter AG, Clandinin TR, and Desplan C (2014). Processing properties of ON and OFF pathways for Drosophila motion detection. Nature 512, 427–430. 10.1038/nature13427. [PubMed: 25043016]
20. Kolodziej PA, Timpe LC, Mitchell KJ, Fried SR, Goodman CS, Jan LY, and Jan YN (1996). Frazzled encodes a Drosophila member of the DCC immunoglobulin subfamily and is required for CNS and motor axon guidance. Cell 87, 197–204. 10.1016/S0092-8674(00)81338-0. [PubMed: 8861904]
21. Cosmanescu F, Katsamba PS, Sergeeva AP, Ahlsen G, Patel SD, Brewer JJ, Tan L, Xu S, Xiao Q, Nagarkar-Jaiswal S, et al. (2018). Neuron-subtype-specific expression, interaction affinities, and specificity determinants of DIP/Dpr cell recognition proteins. Neuron 100, 1385–1400.e6. 10.1016/J.NEURON.2018.10.046. [PubMed: 30467080]
22. Naidu VG, Zhang Y, Lowe S, Ray A, Zhu H, and Li X (2020). Temporal progression of Drosophila medulla neuroblasts generates the transcription factor combination to control T1 neuron morphogenesis. Dev. Biol. 464, 35–44. 10.1016/j.ydbio.2020.05.005. [PubMed: 32442418]
23. Kurmangaliyev YZ, Yoo J, Valdes-Aleman J, Sanfilippo P, and Zipursky SL (2020). Transcriptional programs of circuit assembly in the Drosophila visual system. Neuron 108, 1045–1057.e6. 10.1016/J.NEURON.2020.10.006. [PubMed: 33125872]

24. Özel MN, Gibbs CS, Holguera I, Soliman M, Bonneau R, and Desplan C (2022). Coordinated control of neuronal differentiation and wiring by sustained transcription factors. Science 378, eadd1884. 10.1126/science.add1884. [PubMed: 36480601]

25. Takemura SY, Bharioke A, Lu Z, Nern A, Vitaladevuni S, Rivlin PK, Katz WT, Olbris DJ, Plaza SM, Winston P, et al. (2013). A visual motion detection circuit suggested by Drosophila connectomics. Nature 500, 175–181. 10.1038/nature12450. [PubMed: 23925240]

26. Peng J, Santiago IJ, Ahn C, Gur B, Tsui CK, Su Z, Xu C, Karakhanyan A, Silies M, and Pecot MY (2018). Drosophila FEZF coordinates laminar-specific connectivity through cell-intrinsic and cell-extrinsic mechanisms. Elife 7, e33962. 10.7554/ELIFE.33962. [PubMed: 29513217]

27. Moore SW, Zhang X, Lynch CD, and Sheetz MP (2012). Netrin-1 at-tracts axons through FAK-dependent mechanotransduction. J. Neurosci. 32, 11574–11585. 10.1523/JNEUROSCI.0999-12.2012. [PubMed: 22915102]

28. Sato A, and Tomlinson A (2007). Dorsal-ventral midline signaling in the developing Drosophila eye. Development 134, 659–667. 10.1242/dev.02786. [PubMed: 17215299]

Highlights

- Netrin pathway has multiple roles in guidance of fly medulla visual projection axons
- Early-born Tm neurons require Fra/Netrin signaling to pioneer the targeting path
- Fra functions in lobula branch extension of TmY3 and layer- specific targeting of Tm3
- Diffusible Netrin is required for axon targeting of fly medulla projection neurons

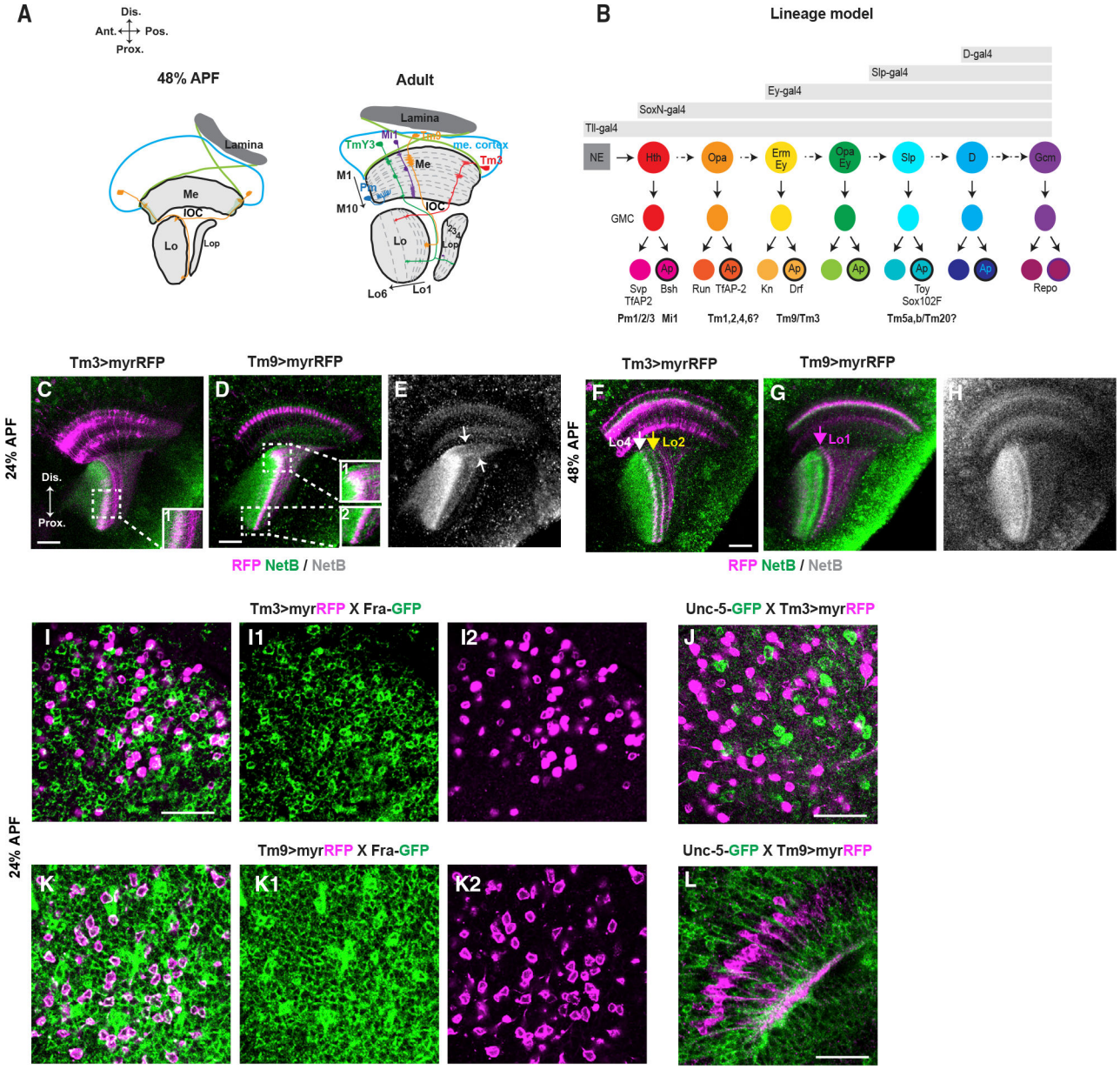

Figure 1. Tm3 and Tm9 axons target lobula progressively during development

(A) A schematic drawing of the optic lobe at 48% APF and adult. IOC, inner optic chiasm; Me, medulla; Lo, lobula; Lop, lobula plate. At the 48% APF stage, Tm axons from posterior younger columns cross anterior axon bundles to target lobula, forming the IOC. The individual medulla columns are exemplified in green shadow. At the adult stage, neuropil layers are numbered, and representative neural types are labeled.

(B) The temporal cascade of medulla neuroblasts. Some temporal stages are skipped for simplicity. Expression windows of various Gal4 lines, relevant neural transcription factors, and exemplified neuron types known before this work are shown.

(C–E) 24% APF brains. NetB (green in C and D, gray in E) is enriched throughout the lobula neuropil.

(C and C1) Tm3 (purple) from early-born anterior medulla columns arrive at the proximal part of lobula, and Tm3 from late-born posterior medulla columns have not arrived at the lobula. All arrived Tm3 show the bushy growth cone morphology.
(C1) A magnified view of the dashed square in (C).
(D) All Tm9 axons (purple) arrive at the lobula. Tm9 terminals at the distal lobula (magnified box 1) show the bushy growth cone morphology and are colocalized with NetB. Tm9 terminals at the proximal lobula show the mature cylinder shape (magnified box 2) and are not colocalized with NetB (green).
(E) Arrows point to the gradient of NetB localized in the cleft.
(F–H) 48% APF brains. NetB (green in F and G, gray in H) is distributed at specific layers.
(F) NetB is enriched in M3, Lo2 (yellow arrow), and Lo4–Lo6. The white arrow marks Lo4. All Tm3 (purple) arrive at the lobula and show two arbors at Lo2 and Lo4, which colocalize with a high NetB signal.
(G) All Tm9 (purple) show cylinder-like terminals at Lo1 (purple arrow). Note: this driver also labels non-Tm9 neurons.
(H) Distribution of NetB at lobula.
(I–L) 24% APF brains.
(I–I2) Tm3 (purple) express Fra-GFP (green).
(J) Tm3 (purple) do not express Unc-5-GFP (green).
(K–K2) Tm9 (purple) express Fra-GFP (green).
(L) Tm9 (purple) do not express Unc-5-GFP (green).
Scale bars: 20 μm.

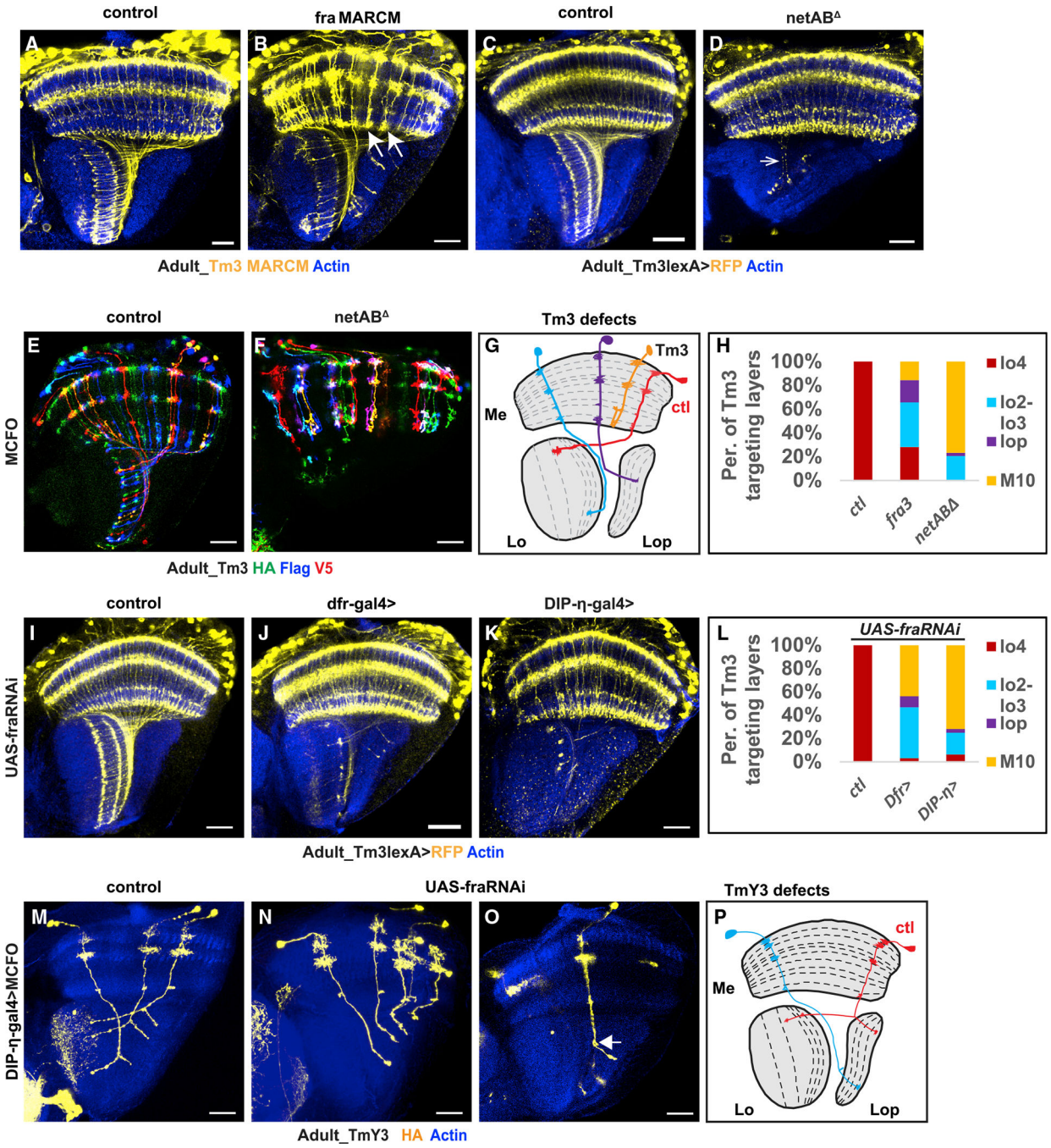

Figure 2. Fra acts non-cell-autonomously for Tm3 to leave the medulla neuropil

(A and B) MARCM is used to label Tm3 (yellow) within recombined control clones (A) or *fra* mutant clones (B). Note: recombination efficiency is high.

(B) Representative Tm3 axons stalled at M10 are marked by white arrows.

(C and D) Tm3 are labeled by *Tm3-lexA > lexop-tdTomato* (yellow).

(C) Wild-type Tm3.

(D) Tm3 targeting in *netAB* double mutants. Most Tm3 axons do not leave the medulla neuropil, and the lobula integrity is disrupted in *netAB* mutants. Arrow points to Tm3 axons that leave the medulla but fail to form the IOC.
(E and F) MCFO is used to label individual Tm3.
(E) Wild-type Tm3.
(F) Tm3 in *netAB* mutants. Most Tm3 stop at M10, and their axons turn back to the medulla, forming the hook structure.
(G) Schematic of wild-type Tm3 (red) and abnormal Tm3 (all other colors) shown in (B), (D), and (F).
(H) Quantification of the percentage of Tm3 axons that targeted Lo4, Lo2–Lo3, Lop, and M10 in wild type, *fra* MARCM, and *netAB* double mutants, as shown in (A)–(D).
(I–K) Tm3 are labeled by *Tm3-lexA, lexop-tdTomato*.
(I) Wild-type Tm3.
(J) Knocking down Fra using *Dfr-Gal4* results in 44% of Tm3 stalled at M10.
(K) Knocking down Fra using *DIP-η-Gal4* results in 72% of Tm3 stalled at M10.
(L) Quantification of the percentage of Tm3 axons that targeted Lo4, Lo2–Lo3, Lop, and M10 in (I)–(K).
(M–O) MCFO is used to label individual TmY3. *DIP-η-Gal4* are expressed in various neurons, including TmY3. TmY3 is identified based on morphology.
(M) Wild-type TmY3. Each TmY3 shows one lobula branch and one Lop branch.
(N) Knocking down fra results in a tiny lobula branch, while the Lop branch is normal.
(O) A tiny lobula branch is marked by the white arrow.
(P) Schematic of wild-type TmY3 (red) and the TmY3 defect in (N) and (N1) (blue).
Scale bars: 20 μm.

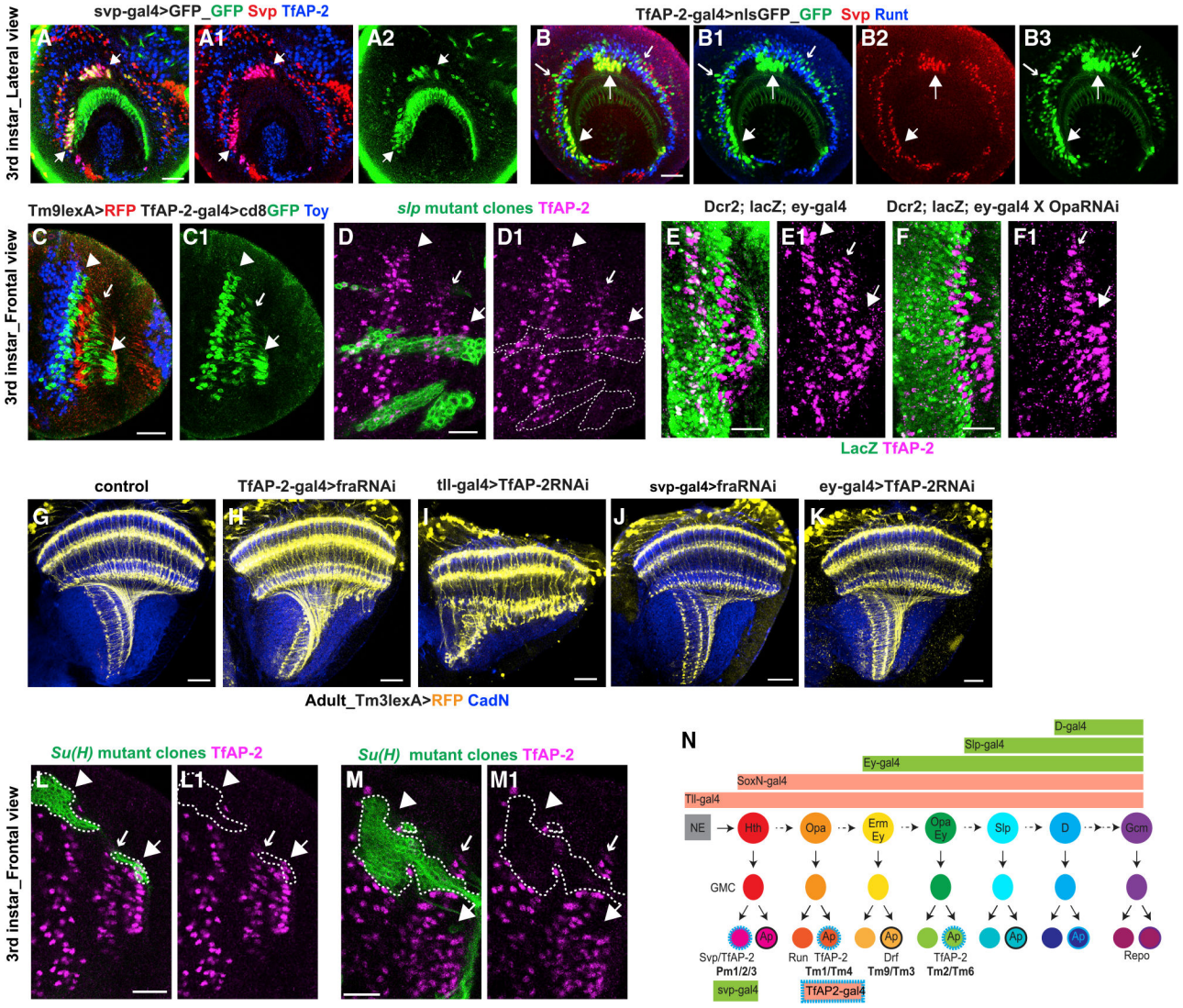

Figure 3. Fra in early-born Tm neurons is required for the IOC formation

(A–A2) Lateral view showing that *svp-Gal4* driving GFP (green) reflects the same expression pattern as anti-Svp (red). Arrows point to Pm neurons that express both Svp and TfAP-2 (blue).

(B–C1) Expression pattern of TfAP-2-Gal4 (GMR24B02-GAL4) at the third-instar larval stage shown in lateral view (B–B3) or frontal view (C and C1).

(B–B3) Big arrow-marked *TfAP-2-Gal4*-expressing neurons (first stripe) are Svp^{+} (red) Pm neurons. Small arrow-marked *TfAP-2-Gal4*-expressing neurons (second stripe) are intermingled with $Runt^{+}$ neurons (blue), suggesting that they are born in the first Opa window. The third stripe of later-born neurons (marked by arrowhead in C) are not observed at this focal plane.

(C and C1) *TfAP-2-Gal4* driving GFP (green) is expressed in three stripes of neurons marked by big arrow, small arrow, and arrowhead, respectively. *TfAP-2-Gal4* is not expressed in Tm9 (red) or in Toy^{+} neurons (blue).

(D and D1) In *slp* mutant clones marked by GFP in green, all three stripes of TfAP2^{+} medulla neurons are still generated.
(E and E1) The first and second TfAP2 stripes are not marked by eyGal4>LacZ (green), while the third stripe neurons are marked by eyGal4>LacZ.
(F and F1) Knocking down the second Opa stripe with *ey-gal4* leads to the loss of the third TfAP-2 stripe, suggesting that the third TfAP-2 stripe is born at the second Opa temporal window (Opa+Ey window).
(G–K) Tm3 are labeled (yellow).
(G) Tm3 in wild type.
(H) Tm3-marked IOC is disrupted in *TfAP-2-gal4>fraRNAi*.
(I) Tm3-marked IOC is disrupted in *tll-gal4>TfAP-2RNAi*.
(J) Tm3-marked IOC is normal in *svp-gal4>fra-RNAi*.
(K) Tm3-marked IOC is normal in *ey-gal4>TfAP-2RNAi*.
(L–M1) In *Su(H)* mutant clones marked by GFP in green, the first stripe of TfAP2 expression (big arrow) is still present, while the second and third stripes are lost (small arrow and arrowhead).
(N) A schematic summarizing the correlation between temporal patterning and Netrin-dependent IOC formation. Different Gal4 lines were used to drive fra-RNAi, and those that showed IOC defects are marked in light red, while those that did not show IOC defects are marked in green. When TfAP2-gal4 (expressed in three stripes of neurons marked by light-blue dashed outline) was used to drive fra-RNAi, an IOC defect was observed with Tm3 axons. We show that Tm2 and Tm6 are generated in the Opa+Ey stage and are not required for IOC formation. Tm1 and Tm4 are generated in the first Opa stage and are likely the pioneering neurons that establish the IOC.
Scale bars: 20 μm.

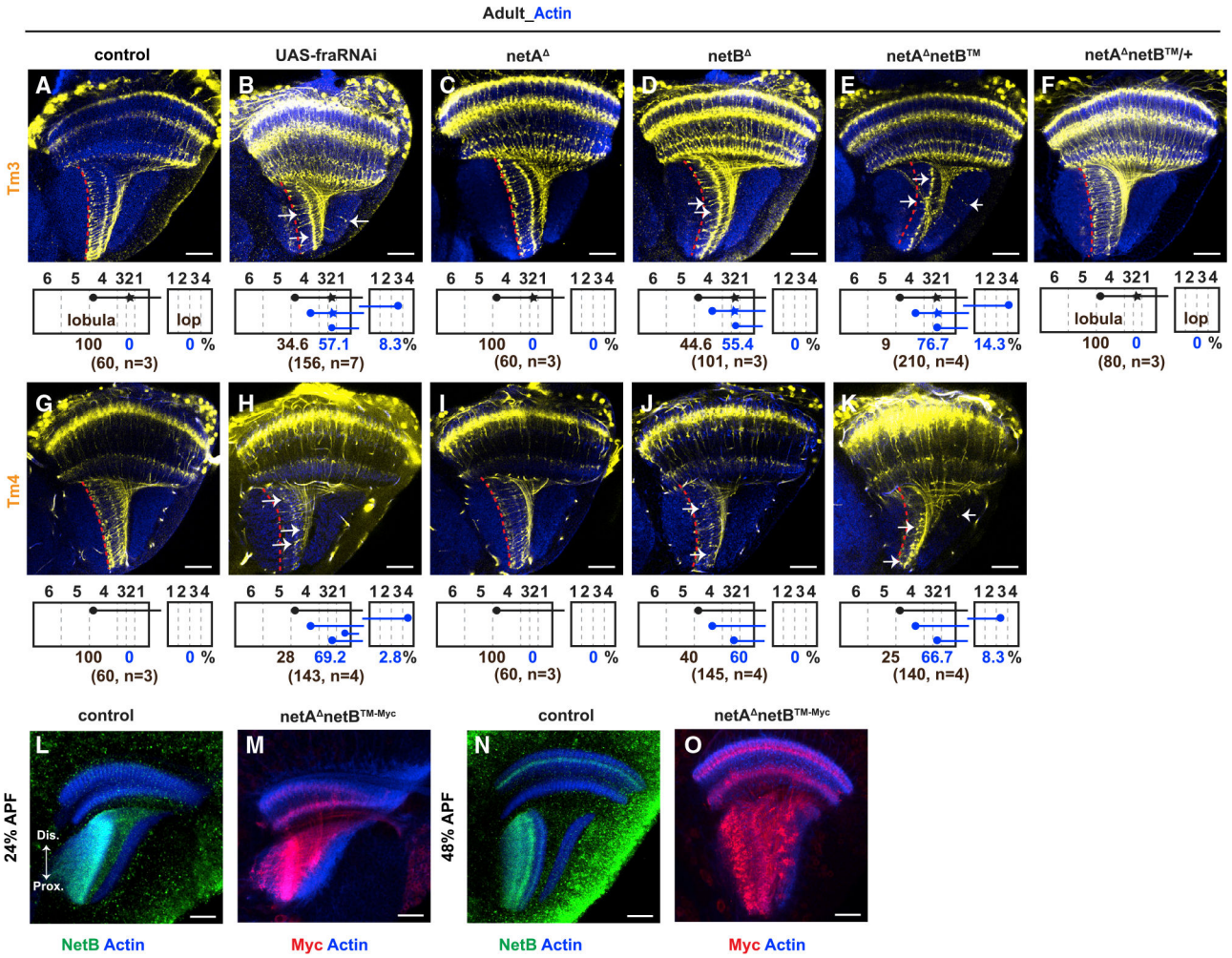

Figure 4. Netrin signaling is required for the layer-specific targeting of Tm3 and Tm4

(A–F) The red dashed line marks the wild-type Tm3 axon targeting layer. Arrows point to examples of mistargeted axon terminals. (A and B) Tm3 are labeled by early *Gal4* (BL76324) driving *UAS-myrRFP* (yellow).

(A) Wild-type Tm3 axons (yellow) arborize at Lo2 and terminate at the boundary of Lo4 and Lo5 (red dashed line).

(B) Knocking down Fra specifically in Tm3.

(C–F) Tm3 are labeled by *Tm3-lexA>lexop-tdTomato* (yellow). Schematic below each image shows the six-layered lobula (left, Lo1–Lo6), four-layered lobula plate (right, Lop1–Lop4), and Tm3 arborization (axon terminals are shown as black or blue dots, and arbors at Lo2 are shown as star). Percentage of targeting layers, total number of counted axons, and the sample size are also shown.

(C) Tm3 targeting in *netA* mutants is normal.

(D) Not all Tm3 axons target lobula layer 4 in *netB* mutants.

(E) Tm3 targeting in membrane-tethered NetB mutants ($NetA^{\Delta}NetB$) is abnormal. Most Tm3 stall at superficial lobula layers. The IOC is also affected.

(F) Tm3 targeting in $NetA^{\Delta}NetB/NetA^{+}NetB^{+}$ is normal.

(G–K) Tm4 are labeled by type-specific *Gal4* with *UAS-mcd8GFP*. Schematic and quantification are shown below. The red dashed line marks the wild-type Tm4 axon targeting layer.

(G) Wild-type Tm4 (yellow) terminate at boundary of Lo4 and Lo5 (red dashed line).

(H) Knocking down Fra specifically in Tm4.

(I) Tm4 targeting in *NetA* mutants is normal.

(J) Not all Tm4 axons target Lo4 in *NetB* mutants.

(K) Tm4 targeting in membrane-tethered NetB (*NetA*^{4}*NetB*) mutants is abnormal. Most Tm4 axons stall at superficial lobula layers.

(L and N) Diffusible NetB (green) of control at 24% or 48% APF.

(M and O) Membrane-tethered NetB (labeled by Myc tag in red) at 24% or 48% APF. They are found in all neuropils.

Scale bars: 20 μm.

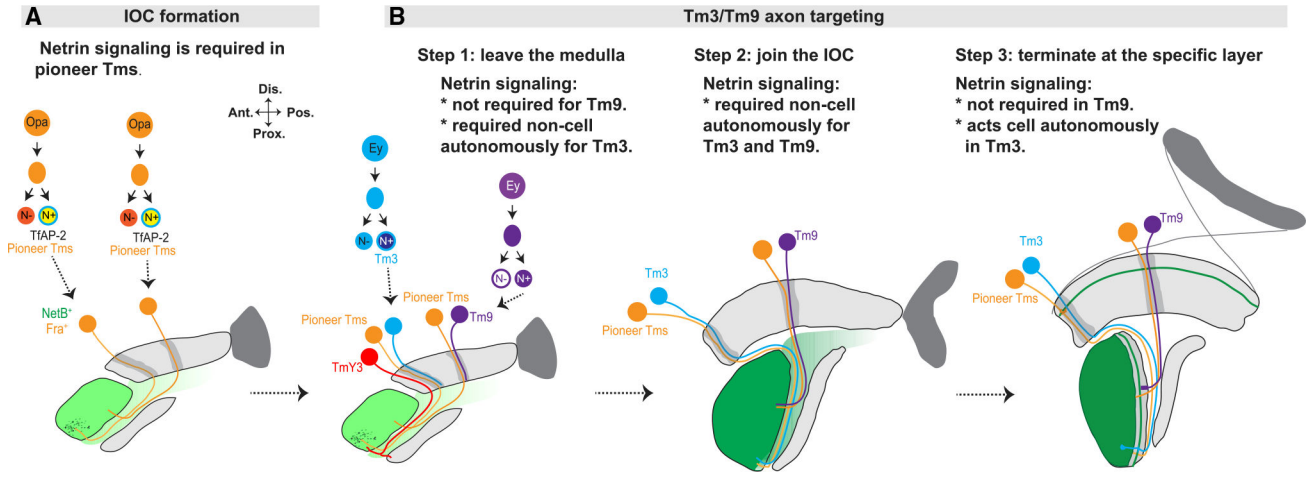

Figure 5. Model of the roles of Netrin pathway in Tm axon guidance

(A) TfAP2-expressing pioneer Tm neurons generated in the first Opa stage target to lobula first within each column. Pioneer Tm neurons from the late-born posterior medulla columns cross all the early-born Tm bundles and form the IOC. Netrin signaling is required in pioneering Tm axons for the IOC establishment.

(B) Later-born Tm neurons within each column such as Tm3 and Tm9 are guided by pioneer Tm axons to target lobula through three steps: leave the medulla, join the IOC, and terminate at the specific layer. Netrin signaling is required differently at different steps of Tm axon targeting. Diffusible Netrin is required for IOC formation and layer-specific targeting of Tm3. Netrin is shown as a gradient in the cleft region. For simplicity, one Tm3 is drawn in one column, and one Tm9 is shown in another column, while they are actually present in each medulla column.

KEY RESOURCES TABLE

REAGENT or RESOURCE	SOURCE	IDENTIFIER
Antibodies		
Mouse anti-Cut	DSHB	Cat# 2B10; RRID:AB_528186
Rat anti-Dfr	M. Sato	N/A
Rat anti-DN-Cadherin	DSHB	Cat# DN-Ex#8; RRID:AB_528121
Rat anti-Flag	Novus	Cat# NBP1-06712; RRID:AB_1625981
Sheep anti-GFP	AbD Serotec	Cat# 4745-1051; RRID:AB_619712
Rabbit anti-HA	Cell Signaling Technology	Cat# #3724; RRID:AB_1549585
Mouse anti-Myc	DSHB	Cat# 9E10; RRID:AB_2266850
Rabbit anti-NetB	B.Altenhein	N/A
Phalloidin-iFluor 405	Abcam	Cat# ab176752; N/A
Rabbit anti-RFP	Abcam	Cat# ab62341; RRID:AB_945213
Guinea-pig anti-Runt	C. Desplan	N/A
Guinea pig anti-TfAP-2	C. Desplan	N/A
Rat anti-Drgx	C. Desplan	N/A
Rat anti-Pdm3	C. Desplan	N/A
Rabbit anti-Mef2	C. Desplan	N/A
Guinea pig anti-Toy	C. Desplan	N/A
Mouse anti-Aop/Yan	DSHB	Cat# 8B12H9; RRID:AB_531807
Mouse anti V5-Tag:DyLightÂ®550	Bio-Rad	Cat# MCA1360D550GA; RRID:AB_2687576)
Donkey Anti-Chicken 647	Jackson ImmunoResearch Laboratories Inc.	Cat# 703-605-155; RRID:AB_2340379
Donkey Anti-Guinea Pig Cy3	Jackson ImmunoResearch Laboratories Inc.	Cat# 706-165-148; RRID:AB_2340460
Donkey Anti-Guinea Pig 488	Jackson ImmunoResearch Laboratories Inc.	Cat# 706-545-148; RRID:AB_2340472
Donkey Anti-Guinea Pig 647	Jackson ImmunoResearch Laboratories Inc.	Cat# 706-605-148; RRID:AB_2340476
Donkey Anti-Mouse 488	Jackson ImmunoResearch Laboratories Inc.	Cat# 715-545-151; RRID:AB_2341099
Donkey Anti-Mouse Cy5	Jackson ImmunoResearch Laboratories Inc.	Cat# 715-175-151; RRID:AB_2340820
Donkey Anti-Mouse Cy3	Jackson ImmunoResearch Laboratories Inc.	Cat# 715-165-151; RRID:AB_2315777
Donkey Anti-Sheep 488	Jackson ImmunoResearch Laboratories Inc.	Cat# 713-545-147; RRID:AB_2340745
Donkey anti-Rabbit 555	Molecular Probes (Thermo Fisher)	Cat# A-31572; RRID:AB_162543
Donkey Anti-Rabbit 488	Jackson ImmunoResearch Laboratories Inc.	Cat# 711-545-152; RRID:AB_2313584
Donkey Anti-Rat Cy3	Jackson ImmunoResearch Laboratories Inc.	Cat# 712-165-153; RRID:AB_2340667
Donkey Anti-Rat Cy5	Jackson ImmunoResearch Laboratories Inc.	Cat# 712-175-153; RRID:AB_2340672
Chemicals, peptides, and recombinant proteins		

REAGENT or RESOURCE	SOURCE	IDENTIFIER
SlowFade Gold	Thermo Scientific	S36936
Deposited data		
The published scRNA-seq data	Konstantinides et al., 2022[15]	GEO: GSE167266
Experimental models: Organisms/strains		
netA$^{\Delta}$	B. J. Dickson	N/A
netB$^{\Delta}$	B. J. Dickson	N/A
netA$^{\Delta}$*B*^{TM}	B. J. Dickson	N/A
netA$^{\Delta}$ *B*$^{\Delta}$	B. J. Dickson	N/A
unc-5-GFP	BDSC	64547
fra-GFP	BDSC	59835
UAS-fra RNAi	BDSC	40826
FRTG13, fra^{3}	BDSC	8813
UAS-TfAP2 RNAi	VDRC	v101552
UAS-Opa RNAi	VDRC	v101531
FRT40A, Su(H)$^{\Delta 47}$*/CyO*	F. Schweisguth	N/A
ey-Gal4	BDSC	48737
slp-Gal4	BDSC	49923
D-Gal4	BDSC	47855
tll-Gal4	BDSC	49694
dfr-Gal4	M. Sato	N/A
DIP-η-Gal4	BDSC	90318
TfAP-2-Gal4	BDSC	49312
Adult: Tm3-Gal4	BDSC	48569
Larval: Tm3-Gal4	BDSC	76324
Tm3-LexA	BDSC	52459
Tm4-Gal4	BDSC	49922
Tm9-Gal4	BDSC	48050
Tm9-LexA	BDSC	54982
UAS-myrRFP	BDSC	7118
MCFO	BDSC	64085
ywhsFLP UASCD8GFP; FRT G13/Cyo; Tm3-Gal4/ TM6B	This study	N/A
Software and algorithms		
Zen	Carl Zeiss	https://www.zeiss.com/microscopy/en/products/software/zeiss-zen.html
R (version 4.0.3)	CRAN	https://www.r-project.org/
Seurat (version 3.2.3)	Satija Lab and Collaborators	https://satijalab.org/seurat/
Photoshop 2021	Adobe	https://www.adobe.com/cy_en/products/photoshop.html

REAGENT or RESOURCE	SOURCE	IDENTIFIER
Illustrator 2021	Adobe	https://www.adobe.com/products/illustrator.html